

In Vitro and In Vivo Tissue Repair With Laser-Activated Chitosan Adhesive

A. Lauto,^{1,5*} M. Stoodley,³ H. Marcel,² A. Avolio,¹ M. Sarris,⁴ G. McKenzie,⁴ D.D. Sampson,⁵ and L.J.R. Foster²

¹Graduate School of Biomedical Engineering, The University of New South Wales, 2052 New South Wales, Sydney, Australia

²School of Biotechnology and Biomolecular Sciences, The University of New South Wales, 2052 New South Wales, Sydney, Australia

³Prince of Wales Medical Research Institute, The University of New South Wales, 2052 New South Wales, Sydney, Australia

⁴School of Medical Sciences, The University of New South Wales, 2052 New South Wales, Sydney, Australia

⁵Optical & Biomedical Laboratory, School of Electrical, Electronic and Computer Engineering, The University of Western Australia, 6009 Western Australia, Australia

Background and Objectives: Sutures are currently the gold standard for wound closure but they are still unable to seal tissue and may induce scarring or inflammation. Biocompatible glues, based on polysaccharides such as chitosan, are a possible alternative to conventional wound closure. In this study, the adhesion of laser-activated chitosan films is investigated in vitro and in vivo. In particular we examine the effect of varying the laser power, as well as adding a natural cross-linker (genipin) to the adhesive composition.

Study Design/Materials and Methods: Flexible and insoluble strips of chitosan films (surface area ~ 34 mm², thickness ~ 20 μ m) were bonded to sheep intestine using several laser powers (0, 80, 120, and 160 mW) at 808-nm wavelength. The strength of repaired tissue was tested by a calibrated tensiometer to select the best power. A natural cross-linker (genipin) was also added to the film and the tissue repair strength compared with the strength of plain films. The adhesive was also bonded in vivo to the sciatic nerve of rats and the thermal damage induced by the laser assessed 4 days post-operatively.

Results: Chitosan adhesives successfully repaired intestine tissue, attaining a maximum repair strength of 14.7 ± 4.3 kPa ($n = 30$) at the laser power of 120 mW. The chitosan-genipin films achieved lower repair strength (9.1 ± 2.9 kPa). The laser caused partial demyelination of axons at the site of operation, but the myelinated axons retained a normal morphology proximally and distally.

Conclusions: The chitosan adhesive effectively bonded to tissue causing only localized thermal damage in vivo, when the appropriate laser parameters were selected. *Lasers Surg. Med.* 39:19–27, 2007. © 2006 Wiley-Liss, Inc.

Key words: biomaterials; tissue welding; tissue engineering

INTRODUCTION

The use of sutures is essential and undisputedly the optimal solution for closure of a wide variety of simple

wounds. However, in many instances the suture is either unable to effect repair or the repair that occurs interferes with the functional rehabilitation of the site. Examples of this include closure of lung tissue following resection (air leakage), nerve repair (scarring and lack of conduction), abdominal repairs (leading to adhesions), and traumatic injuries (agglomeration of many small lesions) [1–4]. In these cases, various surgical glues and adhesives have often been used as alternatives. These include fibrin glues, polymer adhesive based on cyanoacrylates (Dermabond), and albumin (protein) solders; the last are usually activated by lasers. All of these approaches have problems ranging from lack of strength (fibrin glue), tissue toxicity (cyanoacrylates), associated damage from cross-linking systems (UV light), and tissue thermal damage from laser-assisted solders [5–7]. Of particular interest are photochemically activated chitosan gels that have been shown to induce no thermal damage to tissue and to produce better sealing for air leaks than fibrin [8,9]. For example, Ono et al. introduced lactose and azide moieties in the chitosan structure (Az-CH-LA), which was more soluble in water than chitosan at neutral pH. Az-CH-LA aqueous solution was gelatinized by UV irradiation that produced an insoluble hydrogel in 60 seconds. Compared to the fibrin glue, the Az-CH-LA glue sealed more effectively the air leakage from pinholes in isolated small intestine (8.1 vs. 6.8 kPa) and aorta (26.7 vs. 10.7 kPa) and from incisions in

Contract grant sponsor: ARC; Contract grant number: DP0345899; Contract grant sponsor: The Engineering Faculty Grant of The University of New South Wales; Contract grant sponsor: “Early Career” University of Western Australia grant.

*Correspondence to: A. Lauto, Graduate School of Biomedical Engineering, The University of New South Wales, 2052 New South Wales, Sydney, Australia.

E-mail: antoniol@gsbme.unsw.edu.au; a_lauto@hotmail.com

Accepted 5 September 2006

Published online 25 October 2006 in Wiley InterScience

(www.interscience.wiley.com).

DOI 10.1002/lsm.20418

isolated trachea (10.1 vs. 5.6 kPa) [8]. In a recent study, chitosan adhesive films have also been proven to adhere on sheep intestine with shear strength of ~ 14 kPa without any chemical modification and with the use of infrared instead of UV light [10]. In this study, we continue to investigate chitosan adhesive films and explore the impact on the tissue repair strength of varying the laser power as well as varying the adhesive composition by adding genipin, which is a natural cross-linker. Genipin has been reported to spontaneously react with amino groups and to cross-link chitosan or collagen; this cross-linking capability may enhance the strength of chitosan adhesion to tissue [11,12]. Chitosan strips were also bonded *in vivo* on the sciatic nerves of rats to study the acute thermal damage induced by the laser.

MATERIALS AND METHODS

Chitosan Adhesive Films

In Group I, deacetylated chitosan ($\geq 85\%$) from crab shells (Sigma, St. Louis, MO) was dissolved to give a concentration of $1.8 \pm 1\%$ w/v in an aqueous solution containing acetic acid (2% v/v) and indocyanine green (IG, 0.02% w/v) [10]. In Group II, an ethanol solution of genipin (10% w/v) was added to the green chitosan gel of Group I to obtain final concentrations of 1% (w/v) genipin and 0.7% (v/v) ethanol (Fig. 1).

All gelatinous chitosan solutions (pH ~ 4.0) were stirred for 6 hours at 4°C before spreading evenly (thickness ~ 2 mm, surface area ~ 12 cm²) over a sterile and dry Perspex plate. The chitosan solutions were then dried for ~ 9 days under clean conditions and atmospheric pressure at 4°C. The resulting chitosan films were carefully detached from the plate without damage and were insoluble in water. A digital micrometer was used to measure the adhesive thickness, which ranged from 15 to 30 μ m. All films were thereafter cut in rectangular strips ($\sim 7.5 \times 4.5$ mm), placed between sterile glass slides to preserve their flat shape and stored in the dark at 4°C.

Genipin was added to the chitosan solution in order to explore a possible enhancement of film adhesion to tissue, as previously demonstrated for albumin solders [13]. The final concentrations of genipin (1%) and ethanol ($\sim 0.7\%$) were suggested by previous studies [11]. Further, 0.7% ethanol concentration likely induces negligible cytotoxicity [13].

Adhesive Optical Attenuation

A UV-Visible spectrophotometer was used to measure the laser attenuation at 808 nm within the films and to observe the attenuation characteristics of the adhesive due to the presence of IG and genipin. The wavelength of 808 nm corresponds to the absorption peak of IG and to the laser radiation used for laser tissue repair (LTR) [14]. Adhesive films were fixed inside a plastic cuvette and placed in the light beam, which scanned the adhesives over the wavelength range of 400–890 nm. The attenuation length (1/e attenuation) was calculated by assuming the validity of Beer's law: $I = I_0 e^{-Lx}$, where I_0 is the incident beam intensity, L is the attenuation length, and x is the film

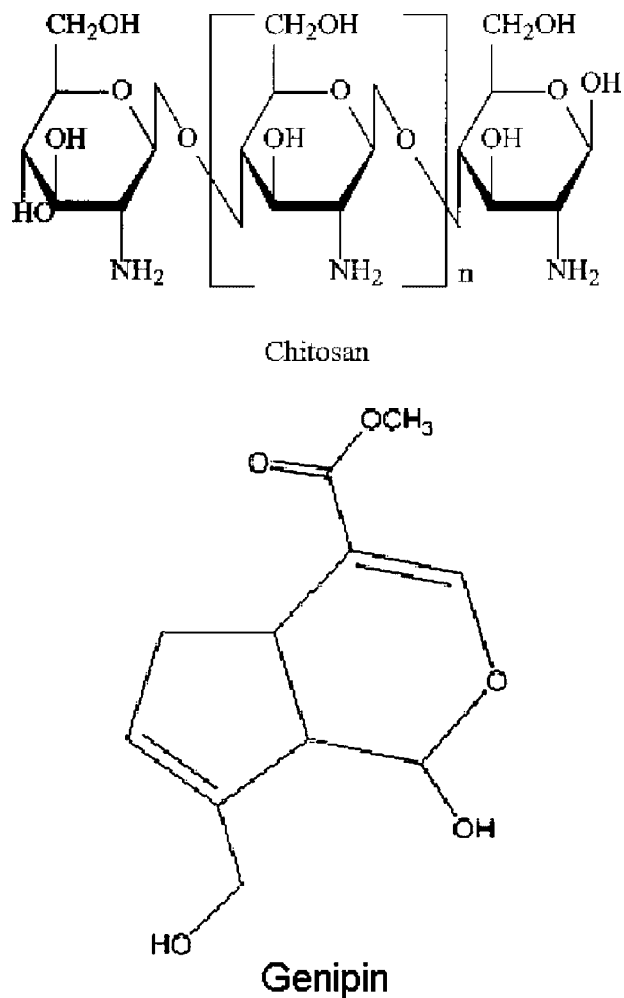


Fig. 1. Molecular structure of chitosan and genipin.

thickness. The attenuation measurements were performed with baseline subtraction.

Laser Tissue Repair (LTR)

Tissue repair was investigated by using a GaAlAs diode laser (Qphotonics, L.L.C., VA), coupled to a multimode optical fiber cable. The fiberoptic cable was inserted in a hand-held probe to provide easy and precise beam delivery by the operator. The laser emitted at 808 nm, with a fiber core diameter of 200 μ m and numerical aperture of 0.22. A Teflon "spacer" was mounted on the fiber probe to ensure the surgeon irradiated tissue from the same distance with a beam spot size of ~ 1 mm. Because the laser is not eye safe (Class IV), safety goggles were worn by all staff in the operating theater.

Fresh intestinal tissue was harvested from sheep immediately after euthanasia and stored at -80°C for 2 weeks. Prior to use, tissue was immersed in deionized water for 15 minutes to defrost and hydrate at room temperature. Intestine sections ($\sim 2 \times 1$ cm) were bisected

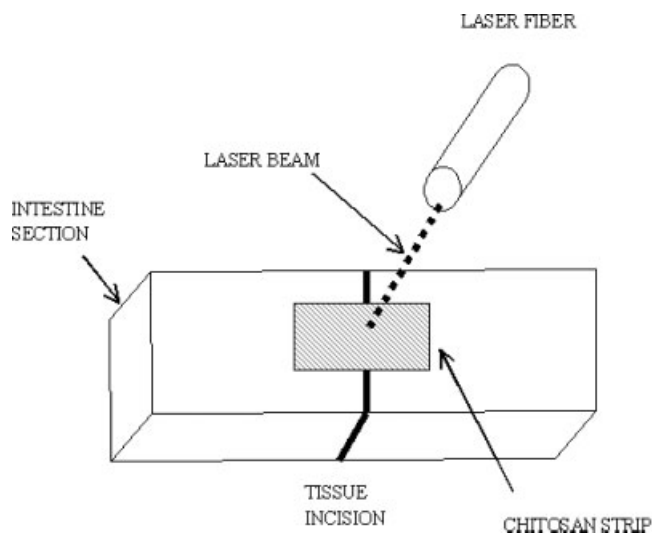


Fig. 2. Schematic top-view of laser tissue repair. A strip of chitosan adhesive is applied across the incision then subsequently irradiated using a laser.

by a full thickness incision with a #10 blade under an operating microscope (20 \times). The intestine was kept moist using deionized water; excess water was absorbed with sterile gauze or cotton tips prior to tissue repair. The incision stumps were approximated end-to-end and a chitosan strip was positioned across the incision on the serosa layer with microforceps ensuring full contact with the intestine. Thereupon, the operator irradiated the adhesive by moving continuously the beam across its surface at a speed of ~ 1 mm/second and without charring or ablating the adhesive (Fig. 2). Sporadic tissue shrinkage under the adhesive was observed during laser irradiation.

In the first part of the experiment, several power levels were used to irradiate the adhesive of Group I in order to select the power associated with the strongest repair (Table 1). For each power level the irradiation time was chosen to keep the fluence constant at 52 J/cm^2 . This latter value provided satisfactory tissue bonding strength and did not disrupt the chitosan film, as previously reported [10]. In

the second part of the experiment, the adhesion strength of chitosan strips from Groups I and II were compared by using the selected power (Table 2). Control tissue repairs were also carried out, applying chitosan strips without the use of laser irradiation.

Tensiometer Measurements

After repair, the tissue was maintained in wet gauze to mimic in vivo conditions and avoid sample desiccation. To assess the strength of the repairs, each sample was tested 10 minutes after repair with a calibrated tensiometer (Instron Mini 55, MA) that was interfaced with a personal computer [10]. A sample was clamped to the tensiometer using pneumatic grips, which were separated at a rate of 22 mm/minute until the adhesive failed. The maximum load at which the adhesive failed was recorded and the shear stress was calculated as the maximum load divided by the adhesive surface area. Based on the tensiometer results, further characterization of the strongest chitosan adhesive among the two groups was carried out, as described in the following sections.

Differential Scanning Calorimetry (DSC)

Thermograms of chitosan strips were obtained by using a differential scanning calorimeter (DSC 7, Perkin-Elmer) to study possible transition phases. The samples (10–15 mg) were accurately weighed into solid aluminum pans and sealed. Heating rates of $10^\circ\text{C}/\text{minute}$ and temperature ranges of $20\text{--}110^\circ\text{C}$ ($n = 14$) were selected for scanning under air with a flow rate of 20 ml/minute. Each scan was repeated twice to thermally stabilize the system and eliminate possible thermogram artifacts. The temperature range was similar to the temperatures ($60\text{--}65^\circ\text{C}$) that are typically achieved during LTR with the chitosan adhesive [10].

Atomic Force Microscopy (AFM)

The surface topography of chitosan adhesives was imaged by using a commercial atomic force microscopy (Digital Instruments Dimension 3000, Urbana, IL). The microscope was operated in tapping mode using silicon cantilevers with a nominal spring constant of 40 N/m and oscillating with average amplitude of 100 nm and a

TABLE 1. Laser Parameters and Adhesive Characteristics ($n = 10$, Mean \pm SD) Are Given for the Repair of Sheep Intestine

Power (W)	Area (mm^2)	Time (seconds)	Irradiance (W/cm^2)	Fluence (J/cm^2)	Shear stress (kPa)
0.16 ± 0.01	22 ± 2	75 ± 11	~ 20	54 ± 4	7.9 ± 2.8
0.12 ± 0.01	23 ± 2	99 ± 6	~ 15	53 ± 1	13.2 ± 3.9
0.08 ± 0.01	22 ± 2	140 ± 11	~ 10	51 ± 2	10.5 ± 4.2
0	34 ± 4	0	0	0	1.3 ± 0.7

Power, laser power during tissue repair; Area, averaged adhesive surface area in contact with the intestine during laser repair; Time, laser irradiation time; Shear stress, maximum load divided by the surface area of the chitosan adhesive.

The chitosan strips had a thickness of $21 \pm 2 \mu\text{m}$.

TABLE 2. Laser Parameters and Adhesive Characteristics ($n = 30$, Mean \pm SD) for the Repair of Rat Intestine

Adhesive group ($n = 30$)	Area (mm^2)	Power (W)	Time (seconds)	Fluence (J/cm^2)	Maximum load (N)	Shear stress (kPa)
Group I + Laser	34 ± 4	0.12 ± 0.01	147 ± 7	52 ± 2	0.50 ± 0.15	14.7 ± 4.3
Group I	34 ± 4	0	0	0	0.07 ± 0.04	1.9 ± 1.3
Group II + Laser	34 ± 4	0.12 ± 0.01	146 ± 4	51 ± 1	0.31 ± 0.10	9.1 ± 2.9
Group II	34 ± 4	0	0	0	0.02 ± 0.01	0.6 ± 0.4

The chitosan strips had a thickness of $20 \pm 5 \mu\text{m}$.

resonance frequency between 200 and 450 kHz. The scanning rate was automatically selected. Surface roughness was calculated as the Z RMS value of the measured vertical displacement:

$$Rq = [\sum_i (Z_i - Z_{\text{ave}})^2 / N]^{1/2}$$

Where Z_{ave} is the average Z value within the scanned area, Z_i is the current Z value, and N is the number of points in the scanned area. Nine measurements of the surface roughness were performed on three separate films; the mean and standard deviation of Rq were also calculated.

Scanning Electron Microscopy (SEM)

In order to visualize the adhesion between the chitosan adhesive and the intestine serosa, segments of small bowel were harvested immediately after sacrificing sheep and stored in phosphate buffer solution at 4°C for half an hour. Tissue sections ($n = 4$) were thereupon repaired as explained previously using the same parameter as listed in Table 2. They were stored in 10% buffered formalin. Subsequently, the sections were cut with a scalpel into small pieces ($\sim 1 \times 2 \text{ mm}$) which were gently washed in 0.1 M phosphate buffer and dehydrated in alcohol at several dilutions (30, 50, and 70% v/v) and then fixed in Karnovsky's solution (2.5% paraformaldehyde and 2% glutaraldehyde in 0.1 M phosphate buffer). The sections were further dehydrated to critical point and sputter coated with Cu before being viewed at 10 kV by scanning electron microscopy (SEM) in high vacuum mode (FEI Quanta 200).

In Vivo Thermal Damage

The thermal damage induced by the laser irradiation of chitosan adhesive was qualitatively assessed in vivo by irradiating chitosan strips placed on rat sciatic nerves. This animal model proved in previous studies to be a reliable test for the safety and efficacy of laser-activated albumin solders, as myelinated axons of peripheral nerves are sensitive to thermal damage [15]. Six adult male Wistar rats, weighing $\sim 600 \text{ g}$, were used in this preliminary study. Approval and consent for the study were obtained in conformity with animal ethical standards.

Anesthesia was induced and maintained during surgery with Isoflurane/ O_2 mix (4% during induction, 2% thereafter) using a standard anesthetic machine. The surgical operation was performed under sterile conditions using a

Zeiss OPMI 7 operating microscope, and the operative procedure was performed under sterile conditions. An oblique skin incision of approximately 3 cm was made in the dorso-lateral part of the right gluteal region. The muscles were gently separated in alignment with their fibers and the sciatic nerves (diameter $\sim 1 \text{ mm}$) exposed at the sciatic notch. The adventitia of the sciatic nerve was partially removed and trimmed with straight microscissors before applying the adhesive; excess water was absorbed with sterile gauze or cotton tips. A chitosan strip (Group I) with a thickness of $\sim 20 \mu\text{m}$ and surface dimensions of $\sim 6 \times 5 \text{ mm}$ was then positioned around the sciatic nerve using microforceps. The chitosan strip adhered fully to the nerve like a collar and assisted with rotation of the nerve, during the procedure (Fig. 3). The laser beam was passed over the length of the strip three times to enhance its adhesion to the epineurium, as described in the previous *LTR section*. The output power, fluence, and beam spot size were $0.12 \pm 0.01 \text{ W}$, $65 \pm 11 \text{ J}/\text{cm}^2$, and $\sim 1 \text{ mm}$, respectively. During laser irradiation, the nerve perineurium was

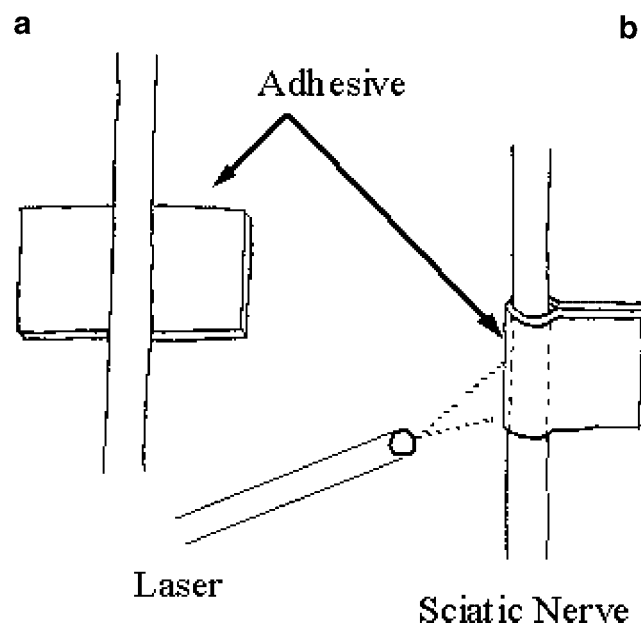


Fig. 3. The adhesive is firstly placed underneath the sciatic nerve (a). The chitosan strip adheres to the nerve like a collar before the laser irradiation takes place (b).

observed to shrink sporadically. Rotation of the nerve was obtained by gently moving the chitosan collar, so that the chitosan strip could be irradiated around the nerve. The redundant chitosan was trimmed from the collar before closing the muscles and the skin with five 3–0 sutures. The animals were thereupon caged individually with no restriction on movement.

Four days after surgery, nerves were harvested at the operated sites, proximal and distal to the adhesive. They were stored in 10% buffered formalin and fixed with Luxol Fast Blue and H&E stained to assess myelinated axons and tissue thermal damage. Sciatic nerves were also harvested from the left gluteal region to serve as controls. At the end of the procedure the animals were sacrificed by an intracardiac injection of 2 ml sodium pentobarbital.

Statistical Analysis

Statistical comparison of means was made using the two-tails unpaired Student's *t*-test and ANOVA one-way and Bonferroni's multiple comparison test at 0.05 level of significance.

RESULTS

Adhesive Attenuation

The attenuation length of the chitosan adhesive with and without IG ($n = 3$, Group I) at 808 nm were respectively $5 \pm 1 \mu\text{m}$ and $228 \pm 72 \mu\text{m}$ (Fig. 4). The presence of genipin in the adhesive (Group II) did not change significantly the attenuation length at 808 nm ($6 \pm 1 \mu\text{m}$, $n = 3$, $P = 0.38$ *t*-test). The attenuation length at 608 nm of the bluish chitosan adhesive with genipin and no IG (Group II) was $6 \pm 2 \mu\text{m}$; the color change of the chitosan strips and the peak absorption signaled cross-linking between genipin and chitosan amino groups. The presence of IG in the adhesive (Group II) did not change significantly the attenuation length at 608 nm ($7 \pm 1 \mu\text{m}$, $n = 3$, $P = 0.54$ *t*-test). Assuming minor scattering and reflection, we may ascribe to IG the efficient absorption of the laser energy at 808 nm inside the chitosan adhesive, independent of the presence of genipin. In contrast, chitosan adhesive without IG weakly attenuated the laser, likely due to scattering. The complete sets of results are reported in Table 3 and Figure 4.

Tensiometer Measurements

First part. The chitosan strips of Group I failed at the tissue interface in all types of repair procedures (Group I). The laser-irradiated strips fully bonded to tissue and adhered more firmly at 80 and 120 mW laser powers (Anova one-way, $n = 10$, $P < 0.001$). Although there was no statistical difference between the shear stress of the adhesive irradiated at 120 and 80 mW (13.2 ± 3.9 kPa and 10.5 ± 4.2 kPa, respectively, $P > 0.05$ Bonferroni's post-test), it appeared that there was a trend towards higher shear stress at 120 mW. The shear stress decreased to 8.0 ± 2.8 kPa at 160 mW laser output; the chitosan strips sporadically burned and twisted during irradiation. Thus, a power level of 120 mW appeared to be the best choice for the second part of the experiment because of the high shear

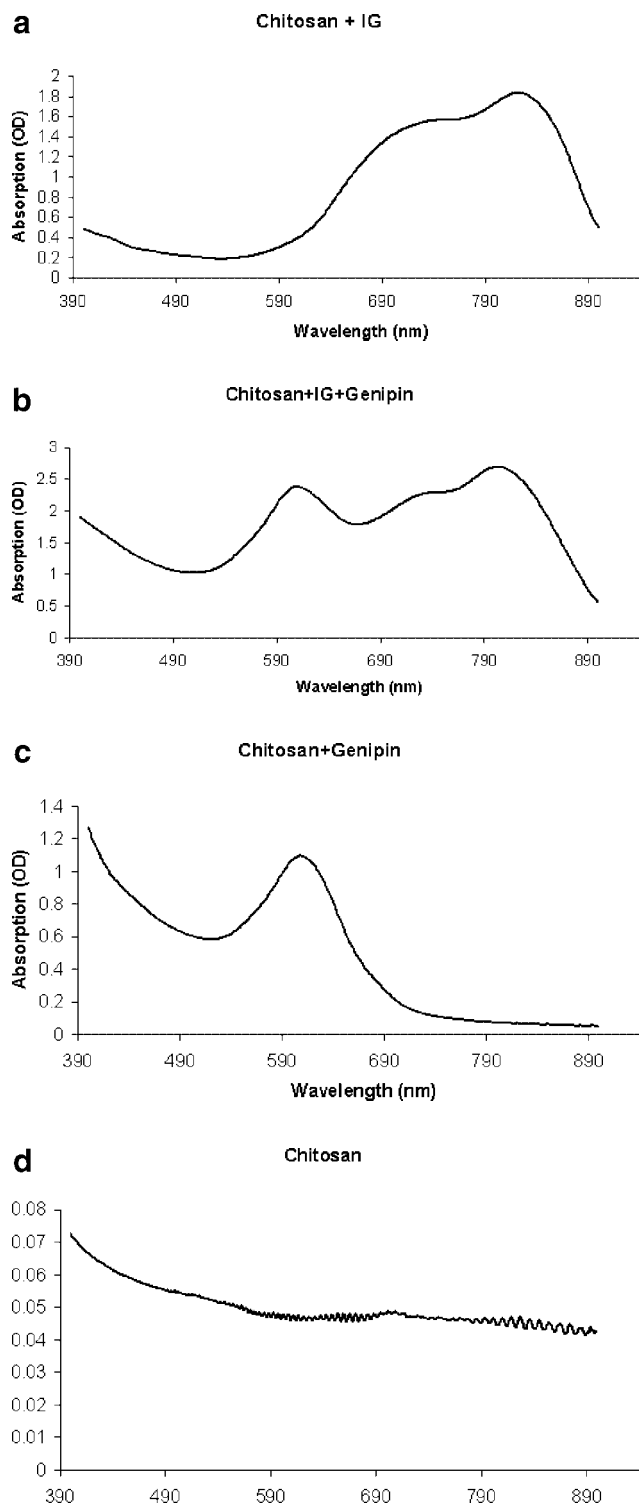


Fig. 4. Typical attenuation spectrum of chitosan adhesive in the visible-NIR region. A strong attenuation peak is localized at 808 nm, corresponding to the well-known absorption wavelength of IG dye (a). Another peak is located at 608 nm due to the genipin cross-linked amino groups (b, c). No peaks are present in chitosan films without IG and Genipin (d).

TABLE 3. Adhesive Attenuation Length at Wavelengths of 808 and 608 nm; the Mean Value \pm the Standard Deviation Are Given

Adhesive type ($n = 3$)	λ (nm)	Thickness range (μm)	Attenuation length (μm)
Chitosan + IG (Group I)	808	20–40	5 ± 1
	608	20–40	25 ± 6
Chitosan	808	20–40	228 ± 72
	608	20–40	223 ± 68
Chitosan + IG + Genipin (Group II)	808	30–50	6 ± 1
	608	30–50	7 ± 1
Chitosan + Genipin	808	10–30	129 ± 16
	608	10–30	6 ± 2

n , number of adhesive samples analyzed. Attenuation length, $1/e$ attenuation of the chitosan adhesive, as calculated from Beer's law. Thickness range, thickness range of chitosan adhesives. The maximum error of the adhesive thickness was $\pm 5 \mu\text{m}$.

stress and reduction in irradiation time. All results are displayed in Figure 5 and Table 1.

Second part. The adhesive with IG (Group I) produced a stronger repair than the adhesive with IG+Genipin (Group II) after laser activation (14.7 ± 4.3 kPa and 9.1 ± 2.9 kPa, respectively, $n = 30$, $P < 0.001$ *t*-test). Strips from the same groups resulted in a significantly lower adhesion to intestine without the laser irradiation step (shear stress = 1.9 ± 1.3 kPa and 0.6 ± 0.4 kPa, $n = 30$, $P < 0.001$, unpaired *t*-test). The strips failed at the tissue interface in all types of repair procedures but for the IG+genipin adhesive (Group II); 30% of the repairs broke the chitosan adhesive in two pieces under the pulling maximum load. Based on their superior adhesive strength, the chitosan strips from Group I were therefore selected for further characterization. All data are displayed in Figure 6 and Table 2.

Differential Scanning Calorimeter

The thermograms of the Group I chitosan strips showed no peak of heat absorption below 110°C but a flat thermal

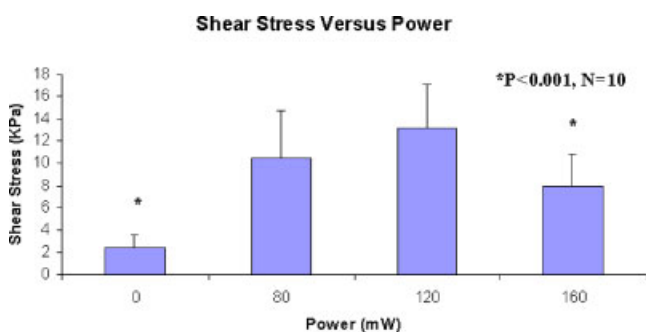


Fig. 5. Histogram of acute shear stress of chitosan adhesive (Group I) versus laser power (mean \pm SD). [Figure can be viewed in color online via www.interscience.wiley.com.]

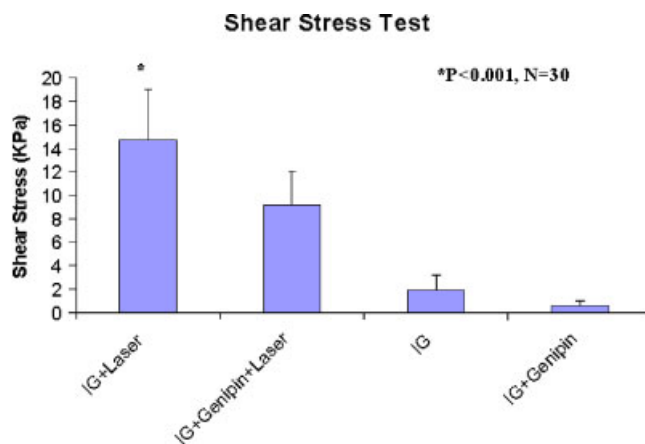


Fig. 6. Histogram of acute shear stress of chitosan adhesives from Groups I and II, with and without the aid of laser radiation (mean \pm SD). [Figure can be viewed in color online via www.interscience.wiley.com.]

profile, therefore no phase transition was observed in this temperature range (Fig. 7).

Atomic Force Microscopy and SEM

The chitosan film surface was relatively smooth ($Rq = 6.7 \pm 4.0$ nm, $n = 9$) with irregular corrugations appearing sporadically. A typical surface topography is shown in Figure 8. The chitosan films were therefore intact with no holes or other apparent defect.

SEM images ($n = 4$) confirmed the chitosan strips adhered to the intestine serosa, even if the adhesion line was sporadically interrupted (Fig. 9).

In Vivo Thermal Damage

The histology of the sciatic nerves showed that some of the axons immediately beneath the irradiated adhesive were demyelinated, indicating potential thermal damage (Fig. 10a,b). The proximal and distal parts of the operated nerve, about 5-mm apart from the irradiated site, appeared

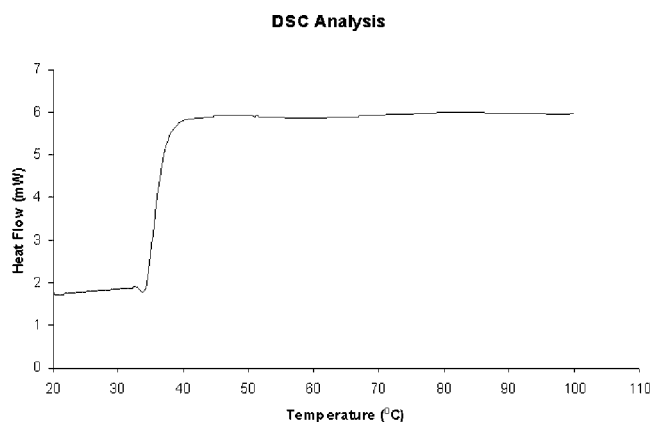


Fig. 7. The DSC scans showed no peaks of heat absorption below 100°C and therefore no phase transition occurred in this temperature range.

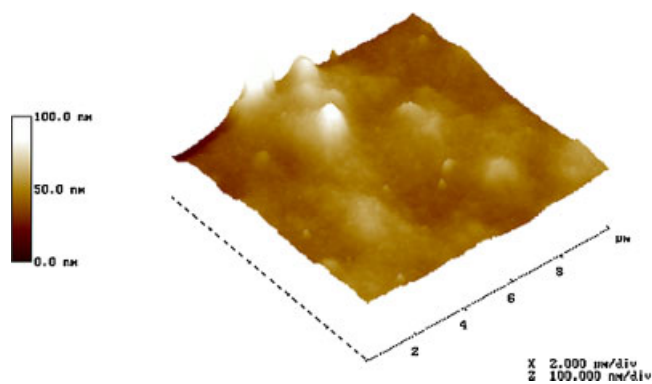


Fig. 8. Three-dimensional map of the adhesive surface recorded by the AFM. The chitosan adhesive appears intact with no holes or other apparent defect. [Figure can be viewed in color online via www.interscience.wiley.com.]

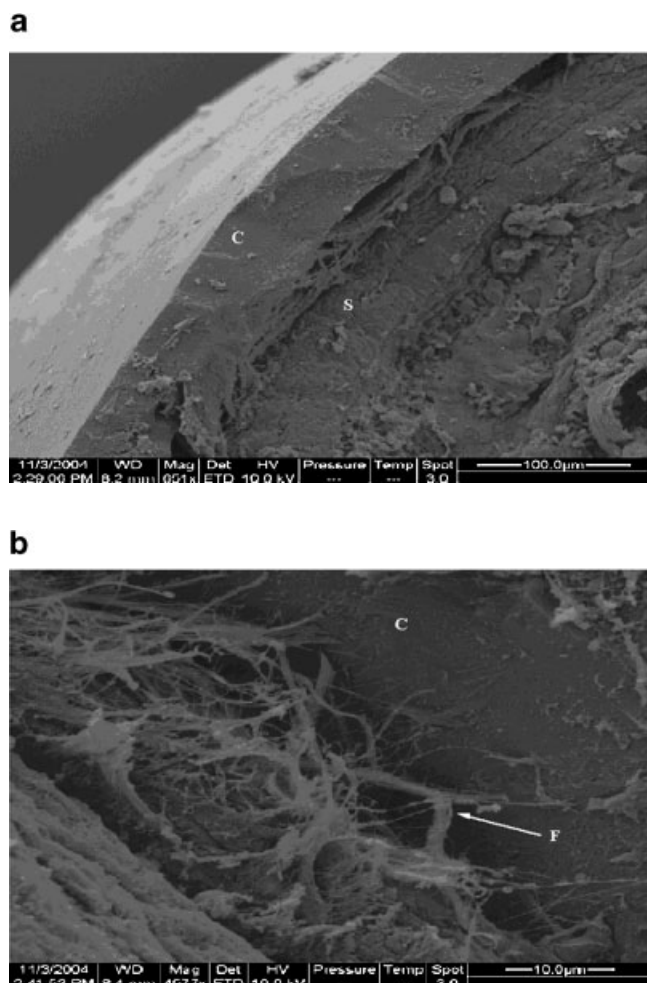


Fig. 9. **a**: SEM cross-section of a chitosan strip (C) bonded to sheep intestine (S). **b**: Particular of (a) at higher magnification. Collagen fibers (F) are clearly bonded on the adhesive (C).

less affected by the heat with the myelinated axons retaining a normal morphology if compared to controls (Fig. 10c–e).

DISCUSSION

Chitosan adhesive strips demonstrated an initial adhesion to tissue prior to laser irradiation (~ 1.9 kPa), which is in agreement with previous reports [16]. The adhesion was greatly enhanced by the laser at a power level of 120 mW. Other laser powers were relatively less efficient in binding

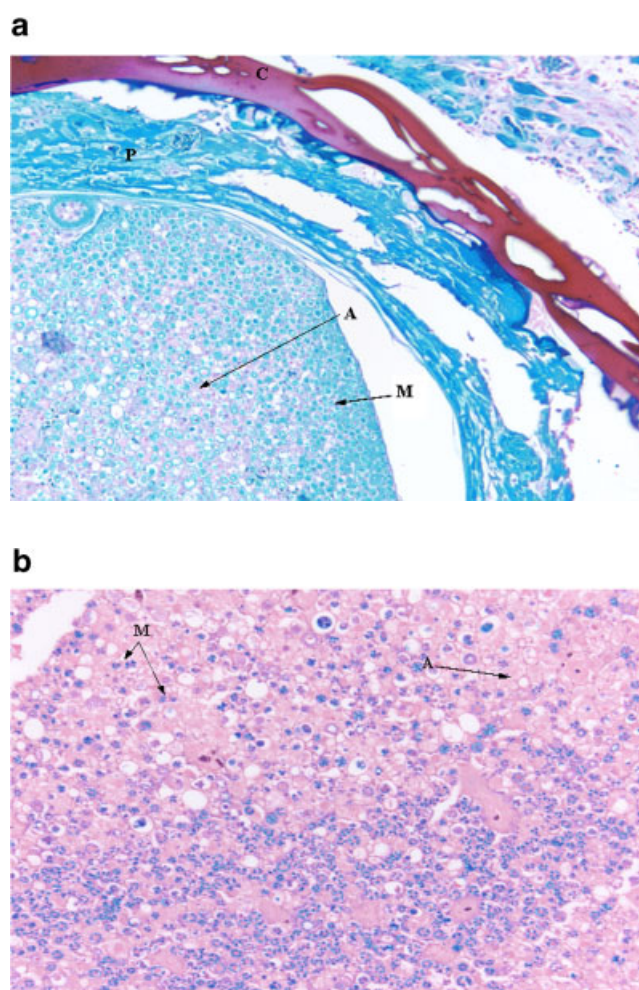


Fig. 10. **a**: Cross-section of an operated nerve. The adhesive (C) was laser-bonded to the perineurium (P); several axons are demyelinated (A) while others preserve the blue myelin sheet (M) 4 days post-operatively (Luxol Fast Blue, 20 \times). **b**: Particular of (a) at higher magnification (Luxol Fast Blue, 40 \times). **c**: Cross-section of the laser-operated nerve at the distal site. Several axons preserve their myelinated sheet (M) while others are demyelinated (A) (Luxol Fast Blue, 20 \times). **d**: Cross-section of the proximal site of the laser-operated nerve. The axons are myelinated and retained their normal morphology (Luxol Fast Blue, 20 \times). **e**: Cross-section of a non-operated sciatic nerve (control). The majority of axons are myelinated (Luxol Fast Blue, 20 \times). [Figure can be viewed in color online via www.interscience.wiley.com.]

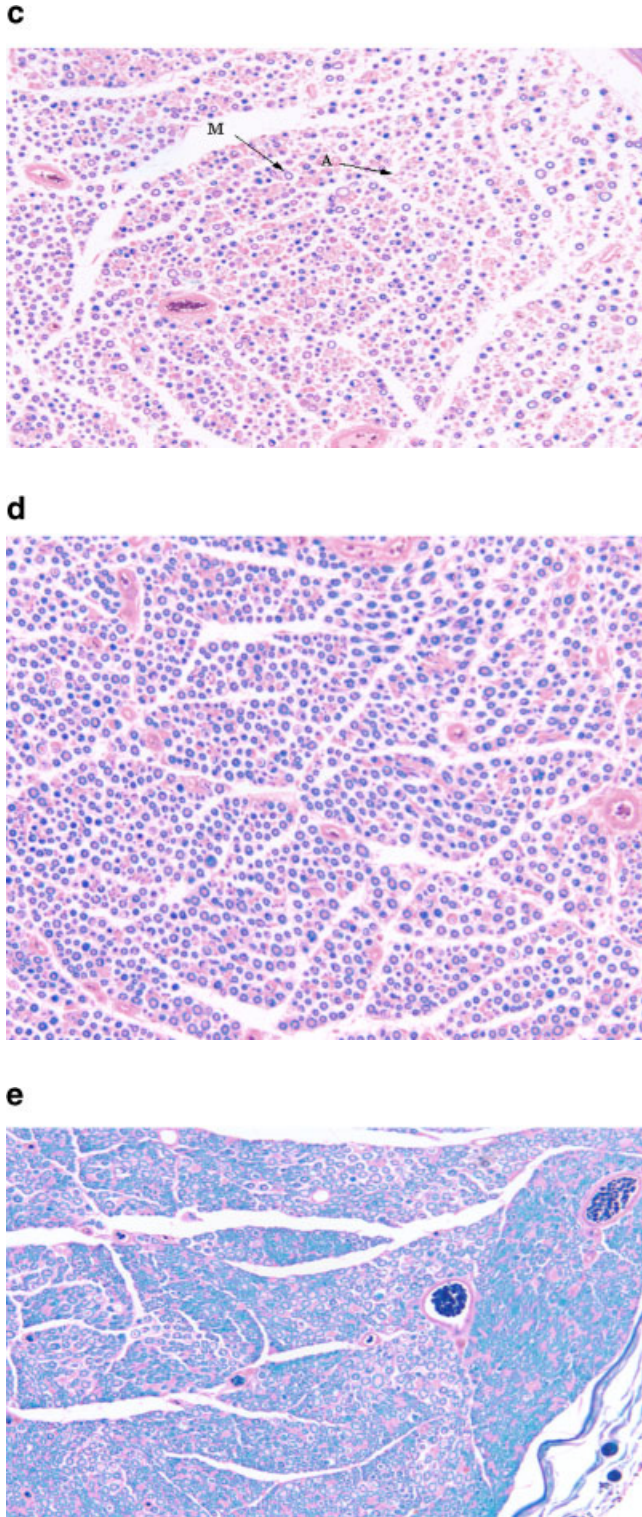


Fig. 10. (Continued)

the chitosan film on tissue. In particular, 160 mW decreased the repair shear strength and 80 mW prolonged the irradiation time without improving the shear strength. The molecular mechanism responsible for this photo-

adhesion is not yet clear, although we may hypothesize that polyanionic–polycationic interactions and hydrogen bonding occurred between collagen and chitosan when the laser generated heat denatured the collagen, as previously reported [17,18]. SEM images confirmed the serosa adhesion to the chitosan film. The bonding strength appeared to decrease if genipin was added to the composition with or without laser activation (~ 9.1 and 0.6 kPa, respectively). Genipin strongly reacted with amino groups of the adhesive as evidenced by the high absorption peak at 608 nm [19]. It may be possible that intermolecular and intramolecular cross-linking impaired the binding capability of collagen and chitosan. The free amino groups of chitosan, for example, might have diminished causing less polyanionic–polycationic interactions and hydrogen bonding with tissue collagen. Genipin also weakened the tensile strength of chitosan films and caused cohesive failure in 30% of the intestine repairs.

In vivo histology showed partial axon demyelination beneath the laser-activated adhesive, 4 days post-operatively. The demyelination was mostly limited to those axons immediately under the adhesive while the majority of axons in the proximal and distal sites were myelinated and preserved their normal morphology. The axon demyelination was likely due to the laser high fluence (~ 65 J/cm²) used to activate the adhesive, even if satisfactory bond strength (~ 11 kPa) was achieved in vitro by using a lower fluence (~ 52 J/cm²). The temperature reached at the tissue interface during LTR is expected to be $\sim 65^\circ\text{C}$, as reported previously [10]. During the procedure, the surgeon irradiated the chitosan strips for longer than necessary because the adhesive activation lacked a visual end point. A reduction in fluence and temperatures are therefore needed to avoid or diminish nerve thermal damage; it also may prove beneficial to irradiate the adhesive with pulses rather than in continuous wave, as previously reported [20].

DSC thermograms showed that chitosan adhesives did not undergo a phase transition when laser activated. Hence, the fluence (~ 52 J/cm²) characterizes the LTR of chitosan adhesives better than the radiation dose (J/mg). In contrast, the latter is more appropriate for albumin solders, which undergo a phase transition during denaturation and they require a fixed amount of energy per mole to change the protein conformation (1.2 ± 0.5 J/g) [21].

The flexibility of the chitosan adhesive permitted the ready manipulation of tissue without fear of breaking or tearing. The adhesive did not fold or breakdown when manipulated with forceps and appeared to be well suited for tissue repair. The application of the adhesive on tissue was also facilitated by its adhesiveness prior to laser activation and hydrophilic properties [10]. For example, the chitosan strip adhered like a collar on the nerve stumps, aligning them end-to-end, and allowing nerve rotation during the laser irradiation.

Further studies are needed to elucidate the mechanism of the chitosan film adhesion to tissue in order to reduce its activation temperature and enhance the repair strength.

The lack of an accepted end-point for lasing the adhesive will also be the subject of future investigations.

REFERENCES

1. Kjaergard HK. Suture support: Is it advantageous? *Am J Surg* 2001;182:15S–20S.
2. Millesi H. Peripheral nerve injuries. Nerve sutures and nerve grafting. *Scand J Plast Reconstr Surg Suppl* 1982;19:25–37.
3. Kramer K, Senninger N, Herbst H, Probst W. Effective prevention of adhesion with Hyaluronate. *Arch Surg* 2002;137:278–282.
4. Pecha RE, Prindiville T, Kotfila R, Ruebner B, Cheung AT, Trudeau W. Gastrointestinal hemorrhage consequent to foreign body reaction to silk sutures: Case series and review. *Gastrointest Endosc* 1998;48(3):299–301.
5. Petratos PB, Felsen D, Trierweiler G, Pratt B, McPherson JM, Poppas DP. Transforming growth factor-beta2 (TGF-beta2) reverses the inhibitory effects of fibrin sealant on cutaneous wound repair in the pig. *Wound Repair Regen* 2002;10(4):252–258.
6. Tseng YC, Hyon SH, Ikada Y. Modification of synthesis and investigation of properties for 2-cyanoacrylates. *Biomaterials* 1990;11:73–79.
7. Fung LC, Mingin GC, Massicotte M, Felsen D, Poppas DP. Effects of temperature on tissue thermal injury and wound strength after photothermal wound closure. *Lasers Surg Med* 1999;25:285–290.
8. Ishihara M, Nakanishi K, Ono K, Sato M, Kikuci M, Saito Y, Yura H, Matsui T, Hattori H, Uenoyama M, Kurita A. Photocrosslinkable chitosan as a dressing for wound occlusion and accelerator in healing process. *Biomaterials* 2002;23:833–840.
9. Ono K, Saito Y, Yura H, Ishikawa K, Kurita A, Akaike T, Ishihara M. Photocrosslinkable chitosan as a biological adhesive. *J Biomed Mater Res* 2000;49:289–295.
10. Lauto A, Hook J, Doran M, Camacho F, Poole-Warren LA, Avolio A, Foster LJ. Chitosan adhesive for laser tissue repair: In vitro characterization. *Lasers Surg Med* 2005;36(3):193–201.
11. Sung HW, Huang RN, Huang LL, Tsai CC, Chiu CT. Feasibility study of a natural crosslinking reagent for biological tissue fixation. *J Biomed Mater Res* 1998;42(4):560–567.
12. Mi FL, Sung HW, SHYU SS. Synthesis and characterization of a novel chitosan-based network prepared using natural occurring crosslinker. *J Polym Sci A: Polym Chem* 2000;28:2804–2814.
13. Lauto A, Foster J, Ferris L, Avolio A, Zwaneveld N, Poole-Warren LA. Albumin-genipin solder for laser tissue-welding. *Lasers Surg Med* 2004;35(2):140–145.
14. Oz MC, Johnson JP, Parangi S, Chuck RS, Marboe CC, Bass LS, Nowygrod R, Treat MR. Tissue soldering by use of indocyanine green dye-enhanced fibrinogen with the near infrared diode laser. *J Vasc Surg* 1990;11(5):718–725.
15. Lauto A, Trickett R, Malik R, Dawes JM, Owen ER. Laser-activated solid protein bands for peripheral nerve repair: An vivo study. *Lasers Surg Med* 1997;21(2):134–141.
16. Needleman IG, Smales FC, Martin GP. An investigation of bioadhesion for periodontal and oral mucosal drug delivery. *J Clin Periodontol* 1997;24(6):394–400.
17. Taravel MN, Domard A. Relation between the physicochemical characteristics of collagen and its interactions with chitosan. I. *Biomaterials* 1993;14(12):930–938.
18. Taravel MN, Domard A. Collagen and its interaction with chitosan. II. Influence of the physicochemical characteristics of collagen. *Biomaterials* 1995;16(11):865–871.
19. Paik Y, Lee C, Cho M, Hahn T. Physical stability of the blue pigments formed from geniposide of gardenia fruits: Effects of pH, temperature, and light. *J Agric Food Chem* 2001;49(1):430–432.
20. Menovsky T, Van Den Bergh Weerman M, Beek JF. Effect of CO(2)-Milliwatt laser on peripheral nerves: Part II. A histological and functional study. *Microsurgery* 2000;20(3):150–155.
21. Lauto A, Stewart R, Ohebshalom M, Nikkoi ND, Felsen D, Poppas DP. Impact of solubility on laser tissue-welding with albumin solid solders. *Lasers Surg Med* 2001;28:44–49.